Progress In Electromagnetics Research Letters, Vol. 111, 121–129, 2023

A Hybrid-Fed Dual-Polarized Patch Antenna with Metasurface Coverage for 5G Applications

Hanhan Guo[1], Dan Zhang[1, *], Yue Juan[1], Zhendong Ding[2], and Jin He[1]

Abstract—A hybrid-fed dual-polarized antenna with matesurface coverage is proposed in this paper, which can be used for 5G mobile communication base station antennas. By placing the two feeding ports on different layers of dielectric plates in an orthogonal manner, and using electromagnetic coupling and slit coupling for feeding respectively, the antenna can achieve inter-port isolation higher than 35 dB in the operating frequency band. In order to widen the bandwidth and obtain higher gain, the metasurface covering unit is loaded above the patch. The metasurface layer contains an array of 5×5 square patch units printed on the top surface of the dielectric plate. The measurement results show that the proposed antenna has an impedance bandwidth of 12% (3.24 to 3.66 GHz). In addition, the antenna obtains a stable gain of about 5.32 dBi at 3.5 GHz. The proposed antenna meets all the requirements of base station antennas and can be a promising candidate for application in 5G base station systems.

1. INTRODUCTION

Microstrip patch antennas are widely used in wireless sensing and radar systems due to many advantages such as small size, light weight, and low profile. It is easy to realize them in processing technology, and to realize special polarization modes such as dual polarization and circular polarization [1]. However, these antennas have the inherent disadvantage of narrow impedance bandwidth, so it is a considerable challenge to extend the bandwidth while maintaining its miniaturization in antenna design [2].

Dual polarizations refer to two mutually orthogonal polarizations. Unlike single polarization antenna, dual polarization antenna can detect, receive, and send signals with two polarization directions perpendicular to each other at the same time. In a mobile communication base station system, dual polarizations gain much attention due to their superior features of reducing multipath fading and enhancing communication channel capacity [3–5]. There are two important evaluation criteria for dual polarized antennas [6]: isolation and cross-polarization.

In [7], excitation is realized by crossed elliptic-H slots in order to create orthogonal $\pm 45^\circ$ polarizations. The antenna has an impedance bandwidth of 18.5%, and the isolation between ports is below -25 dB in desired operating band. The antenna proposed by [8] consists of three stacked layers, which are the feeding layer, a foam layer, and the radiating layer with two orthogonal symmetrical rectangular slots cut in the radiating patch. The measured isolation of the antenna is better than 25 dB across the operating frequency band. In [9], a novel dual-polarized slot-coupled filtering antenna is proposed which reports a printed Jerusalem cross radiator. The isolation between the two ports is better than 23 dB. A novel dual-polarized vector synthetic dipole (VSD) antenna element is first demonstrated in [10], and the antenna can cover the frequency range of 3.2 to 3.9 GHz with inter-port isolation larger than 25 dB.

Received 4 April 2023, Accepted 10 July 2023, Scheduled 1 August 2023

* Corresponding author: Dan Zhang (zhangdan@njfu.edu.cn).

[1] College of Information Science and Technology, Nanjing Forestry University, Nanjing 210037, China. [2] School of Electronic and Optical Engineering, Nanjing University of Science and Technology, Nanjing 210094, China.

Metasurface is a two-dimensional metamaterial structure with significant advantages in polarization control, bandwidth expansion, and gain enhancement due to its sub-wavelength and phase-modulation properties [11]. The improvement of multiple radiation characteristics of antennas by loading metasurface has great advantages and provides new ideas in the research and design of high-performance antennas [12, 13]. The design in [14] not only increases the antenna bandwidth by loading metasurface, but also changes the relative position of the metasurface and microstrip antenna by rotation, thus realizing different polarization modes. By coupling the apertures under the double-layer metasurface, the design of [15] enables the antennas to approach each other's resonant frequencies in two different modes, thus increasing the bandwidth.

In this paper, a low profile broadband dual-polarized antenna is designed, which has particularly excellent isolation performance and good gain in the operating frequency band. In order to obtain high port isolation, the two polarization ports of this antenna are placed orthogonally on different layers of the dielectric and are fed by two different feeding methods, slit coupling and electromagnetic coupling, respectively, and metasurface coverage layer and reflector plate are introduced above and below the radiator to improve the bandwidth and gain. The antenna has an impedance bandwidth of 12% (3.24 to 3.66 GHz), inter-port isolation higher than 35 dB in the operating band, gain up to 5.32 dBi at 3.5 GHz with excellent performance, and can be used as a 5G base station antenna.

2. DESIGN OF THE PROPOSED ANTENNA

2.1. Antenna Geometry

The antenna designed in this paper consists of three parts, which are the metasurface cover, the multilayer hybrid-fed dual-polarized antenna part, and the reflector plate. The structure of the antenna is shown in Fig. 1. The metasurface metal layer is an array of 5×5 square patches printed on the upper surface of an FR4_epoxy dielectric sheet with a relative dielectric constant of 4.4 and a thickness of 2 mm.

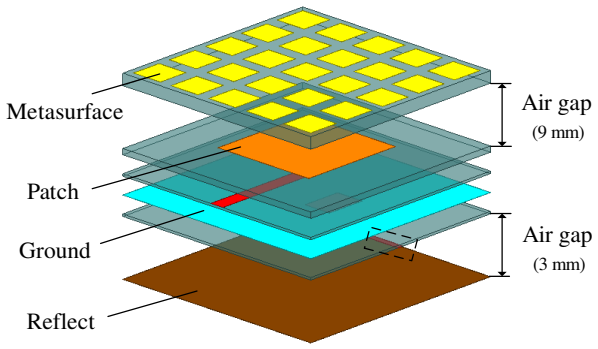

Figure 1. Geometry of the proposed antenna.

The main part of the antenna is composed of three dielectric plates, radiation patch, defective ground, and two vertically placed feeders. The thicknesses of the three dielectric substrates from top to bottom are 1 mm, 0.4 mm, and 0.4 mm in order. There is 9 mm air gap between the metasurface and the multi-layer antenna part, and 3 mm air gap between the reflector plate and the multilayer antenna part. The specific parameters of the antenna are shown in Table 1.

Table 1. Detailed Dimensions (unit: mm).

l_s	l_p	l_m	d_m	l_1	w_1	l_2	w_2	l_3	w_3
38.5	18.6	4.9	2.8	20	2.47	19	1.07	7	5

The radiation patch is on the upper surface of the first dielectric plate. Feed line 1 is located in the middle of the first and second dielectric plates to realize the electromagnetic coupling feed of the vertical polarization port, and feed line 2 is located on the lower surface of the third dielectric plate to realize the gap coupling feed of the horizontal polarization port. Between the second and third layers of the dielectric plate is a metal defect ground with a slit dug out in the middle. The reflector plate is located below the antenna body and is an aluminum plate with a thickness of 0.5 mm. Fig. 2 is a plan diagram of the multilayer structure.

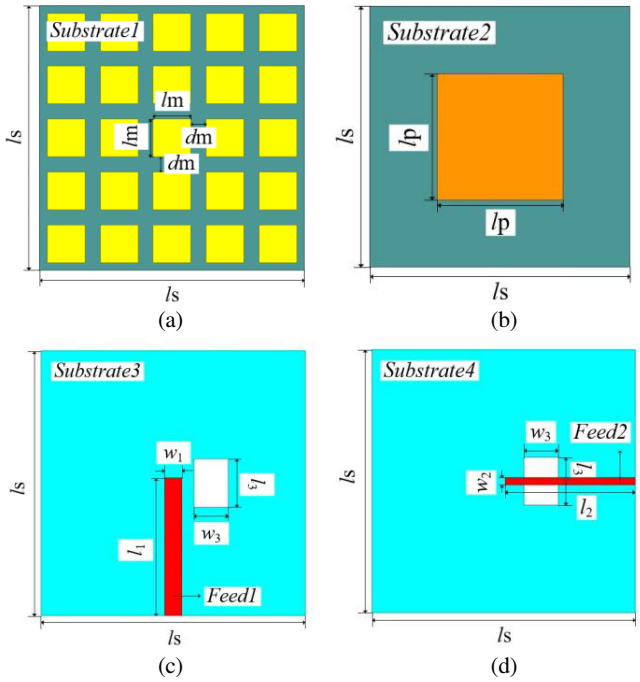

Figure 2. Antenna configuration: (a) top view of the metasurface, (b) top view of the driven patch, (c) top view of the vertical polarization feeder, (d) top view of the horizontal polarization feeder.

2.2. Design Process

In order to clearly understand the design idea of the antenna, the design process of the antenna is shown in Fig. 3.

Firstly, based on the design principle of slot-coupled feed antenna, a slot-coupled dual-polarization antenna with two polarization ports located in the same plane is designed, and the two polarization ports are horizontally and vertically polarized, respectively. This feeding is proposed by Croq and Pozar [16]. It is the use of slit to realize the antenna and feed line electromagnetic coupling, and slot-coupled feeding belongs to the non-contact feeding. Due to the poor isolation between the two ports, the horizontal and vertical polarization ports are considered to be placed on different sides to obtain Ant. 2. However, the port isolation was not significantly improved, so the feed mode of the vertical polarization port has been adjusted from slot coupling feed to electromagnetic coupling feed to obtain Ant. 3.

Loading parasitic units is commonly used to expand the antenna bandwidth, because the parasitic patch can excite the frequency points adjacent to the resonant frequency of the main radiation patch, thus broadening the effective impedance bandwidth. More importantly, the use of parasitic patches broadens the bandwidth of the antenna without seriously affecting the size or degrading the performance of the antenna. In this design, a parasitic element with a square patch parallel to the radiation patch in space is loaded, and Ant. 4 is obtained.

When the metasurface and microstrip antennas are combined, its structure can improve the impedance matching bandwidth of the antenna by exciting the quasi-multiple mode. At the same time, it can be used to improve the antenna gain because it can make the electromagnetic wave reflect

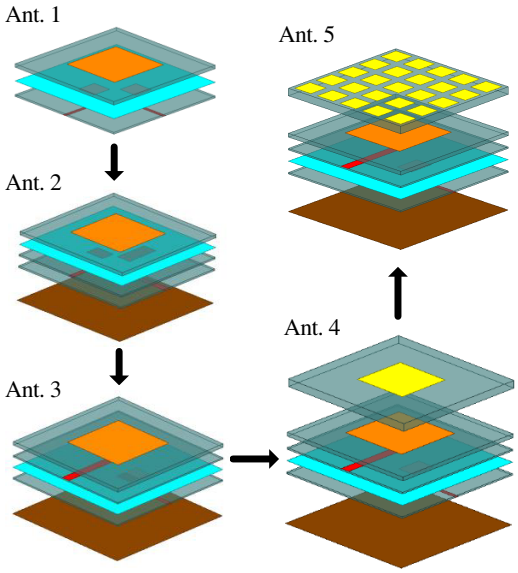

Figure 3. Geometry of Ant. 1 to Ant. 5 (Ant. 1: coplanar slot-coupled dual-polarized antenna; Ant. 2: heterogeneous slot-coupled dual-polarized antenna; Ant. 3: hybrid-fed dual-polarized antenna; Ant. 4: hybrid-fed dual-polarized antenna with parasitic; Ant. 5: hybrid-fed dual-polarized antenna with metasurface).

in the same phase at a specific frequency. This design replaces the parasitic patch on the uppermost plate of Ant. 4 with a metasurface coverage consisting of an array of 5×5 patch units to obtain Ant. 5.

2.3. Results of Simulation

The simulation results of S-parameters of these five antennas are presented in Fig. 4 and Fig. 5.

The first is the performance of antenna bandwidth. It can be seen from Figs. 4(a) and (b) that the resonant frequency of the two feed ports of Ant. 1 is about 3.45 to 3.56 GHz, with a narrow bandwidth of 110 MHz. The resonant frequencies of Ant. 2 and Ant. 3 are very close, 3.38 to 3.58 GHz and 3.39 to 3.60 GHz, respectively, with the bandwidth of 200 MHz and 210 MHz, respectively. The resonant frequency of the two feed ports of Ant. 4 is about 3.35 to 3.64 GHz, and the bandwidth is 290 MHz. The resonant frequency of the two feed ports of Ant. 5 is about 3.24 to 3.66 GHz, and the bandwidth

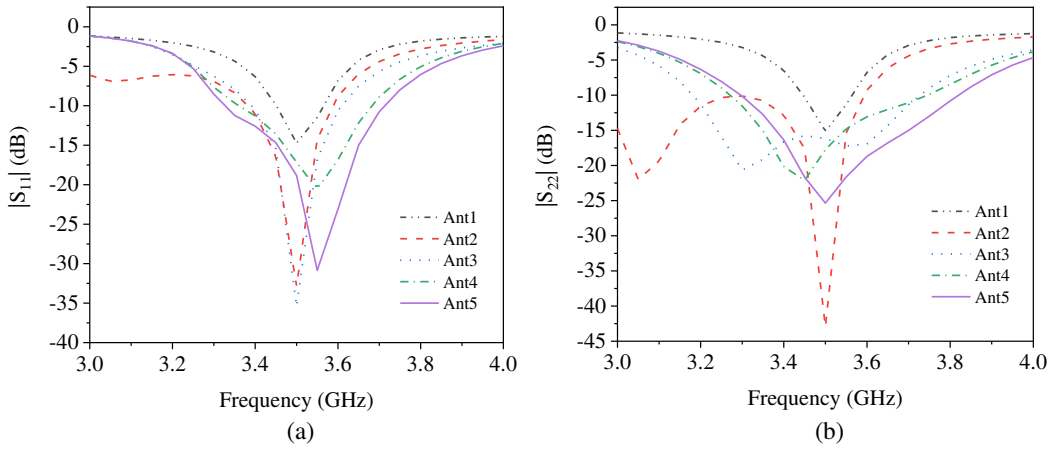

Figure 4. Simulated results for different antennas: (a) $|S_{11}|$, (b) $|S_{22}|$.

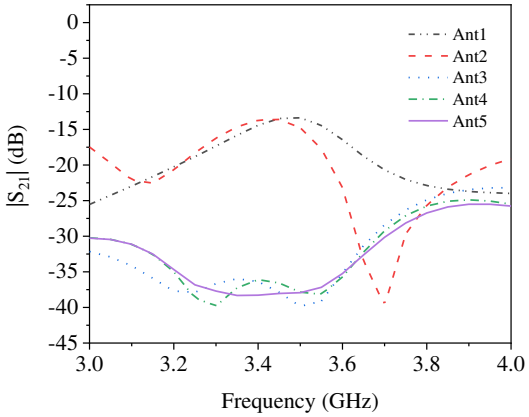

Figure 5. Simulated results for different antennas: $|S_{21}|$.

is 420 MHz. The bandwidth performance of several antennas basically shows an increasing trend, and the relative bandwidth of the final antennas reaches 12%.

The following is the performance of antenna isolation. As can be seen from Fig. 5, the isolation of Ant. 1 and Ant. 2 feed ports in the operating frequency band $|S_{21}|$ is -15 to -20 dB, which indicates that the degree of coupling between the two ports is large, that is, it has a great impact on the electromagnetic coupling efficiency of the antenna, indicating that the method of placing the two polarization ports on the opposite sides of Ant. 2 has little significance for improving the port isolation. By introducing the hybrid feed, the isolation degree between the two polarization ports in the resonant frequencies of Ant. 3, Ant. 4, and Ant. 5 $|S_{21}|$ basically are below -35 dB, which indicates that the degree of coupling between the two ports is small, and the isolation performance is great.

Figure 6 shows the simulation results of the gain patterns of the five antennas. It can be seen that the directivities of the five antennas are basically the same, and the gain increases gradually. The gain of Ant. 1 is only 0.67 dBi. Because a reflector plate is added under the dielectric layer to effectively reflect the energy back, the gain of Ant. 2 is increased to 2.68 dBi, and the gain of Ant. 3 after the introduction of hybrid feed is 3.71 dBi. By introducing heterogeneous parasitic patch and metasurface, respectively, the gain of Ant. 4 and Ant. 5 increases to 5 dBi and 5.7 dBi, respectively, and the final gain of Ant. 5 is very good.

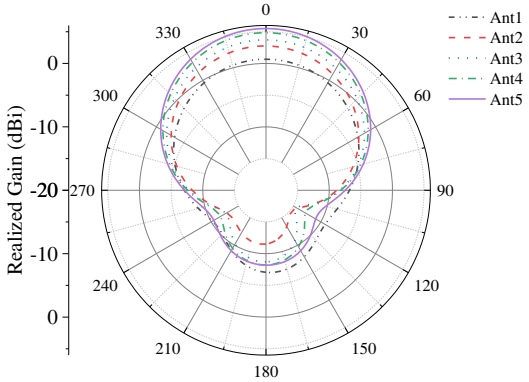

Figure 6. Directional diagram at 3.5 GHz.

Figures 7(a) and (b) show the radiation pattern of the hybrid-feed dual-polarized antenna covered by the super surface at 3.5 GHz on the E plane and H plane, respectively. It can be seen that the cross-polarization ratio of E-plane is 28.7 dB, and the cross-polarization ratio of H-plane is 28.9 dB, which are higher than the performance requirement of 18.0 dB for base station antenna.

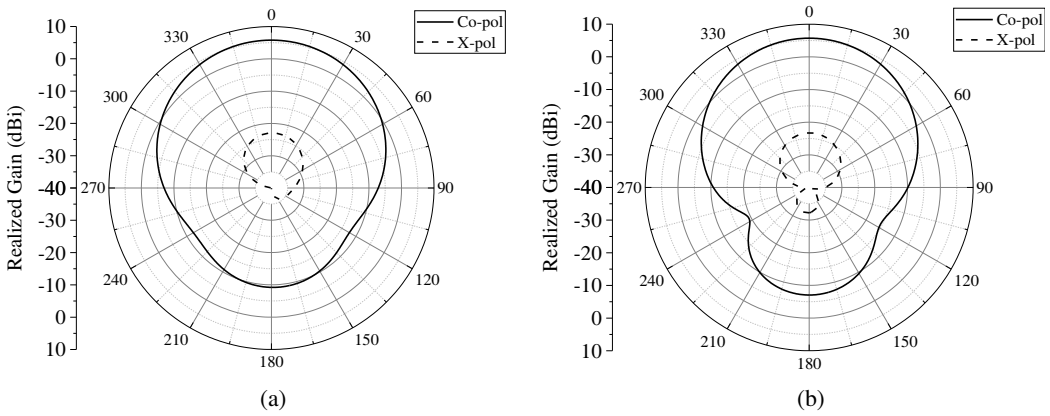

Figure 7. The cross polarization performance: (a) E-plane, (b) H-plane.

2.4. Analysis of Proposed Antennas

Figure 8 shows the current distribution on the surface of the radiation patch and on the feed line when Ant. 2 and Ant. 3 are excited at the vertically polarized port. It can be seen that when the vertical polarization port is excited, the current distribution on the feed line of the horizontal polarization port of Ant. 2 is stronger than that of Ant. 3, indicating that the isolation between the ports of Ant. 2 is low, while the isolation between the ports of Ant. 3 is high. This is because the two feeding ports of Ant. 3 adopt different feeding methods and have a floor to separate them. Therefore, the coupling effect between the two ports is relatively small, and the isolation degree is naturally high.

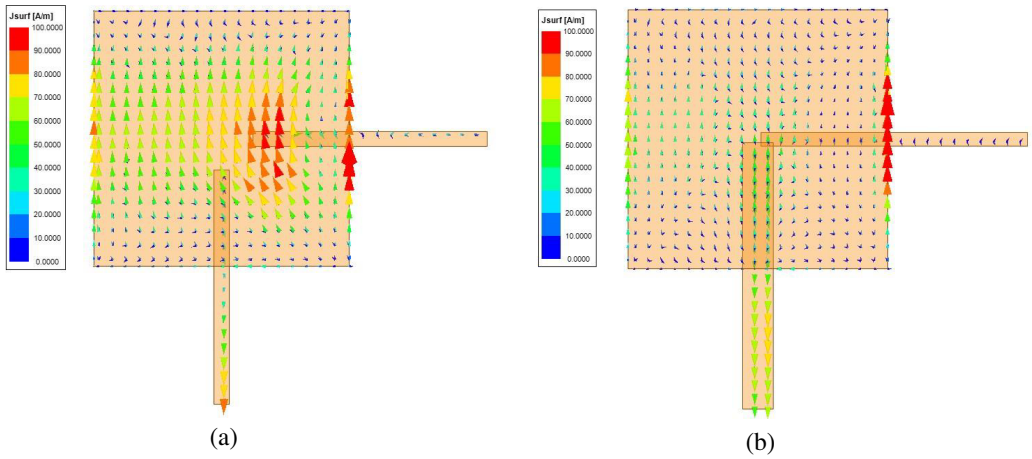

Figure 8. Simulated surface current distribution: (a) Ant. 2, (b) Ant. 3.

Figure 9 shows the surface current distribution on the radiation patch when Ant. 4 and Ant. 5 are excited at the vertically polarized port. It can be seen that the surface current distribution of the radiation patch of Ant. 5 is enhanced compared to that of Ant. 4, which is due to controlling the size of the metasurface and utilizing the in-phase reflection characteristics of electromagnetic waves at 3.5 GHz, and most of the energy is reflected back to the radiation patch for radiation, thereby enhancing the ability of the antenna to directional radiation, i.e., improving antenna gain.

The improvement in antenna gain is due to a better match between the input impedance of the antenna and the characteristic impedance of the feed line, and more energy is reflected back by adding reflector plates and metasurface covering; the improvement in isolation is due to the asymmetric hybrid feed that slightly staggers the resonance of the two ports and has a floor separating the two ports,

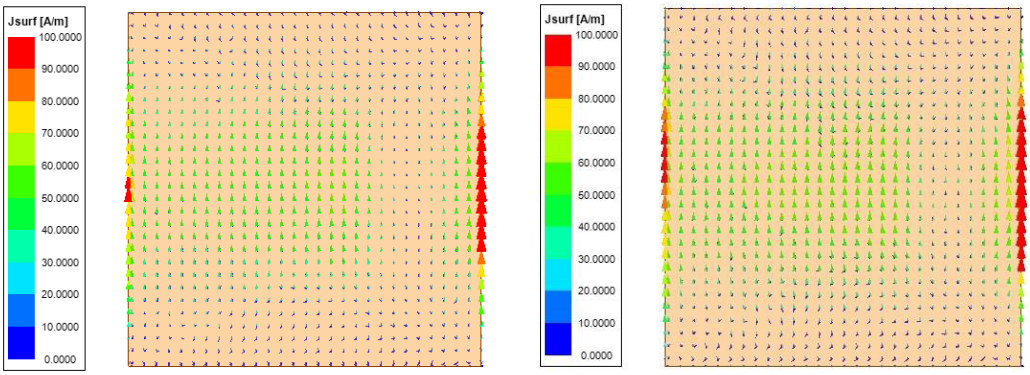

(a) (b)

Figure 9. Simulated surface current distribution: (a) Ant. 4, (b) Ant. 5.

ensuring that less energy leaks out of one port when feeding the other. The improvement of gain and isolation will help to improve the bandwidth of the antenna, because the essence is that when feeding at one port, it can ensure that the most energy is radiated from the radiating patch, and naturally it will get better return loss. Therefore, the impedance bandwidth of the final antenna design is also greatly improved compared to the previous schemes.

3. MEASURED RESULTS

In order to verify the performance of the final design of the hybrid-fed dual-polarized antenna with metasurface coverage, the antenna is processed and tested. As the multilayer structure needs to be assembled during physical test, holes are chosen to be punched in the four corners of the antenna, which are positioned and fixed by plastic screws. The air layer between the antenna body, the meta-surface cover, and the reflector plate is controlled in height by plastic nuts and spacers. In addition, since the SMA head needs to be connected to the test equipment for excitation during the physical test, the three dielectric layers were removed at the edges of the corresponding two feeders to install the SMA head. The prototype and measurement of the proposed antenna are shown in Fig. 10.

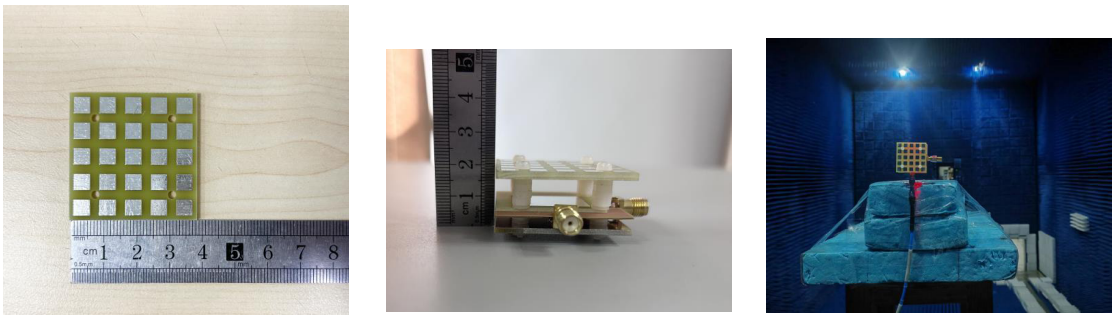

(a) (b) (c)

Figure 10. Photograph of the proposed antenna: (a) top view, (b) side view, (c) measurement in a microwave chamber.

The final comparison of the measured S-parameters, directional diagram, and simulation results are shown in Fig. 11 and Fig. 12. The measured and simulated S-parameters are basically the same; the resonance points of both ports are basically around 3.5 GHz; the resonance frequencies cover 3.35 to 3.70 GHz; and the isolation $|S_{21}|$ is basically below -30 dB in the resonance frequency. The measured and simulated directional diagrams also basically match, with a gain of 5.32 dBi.

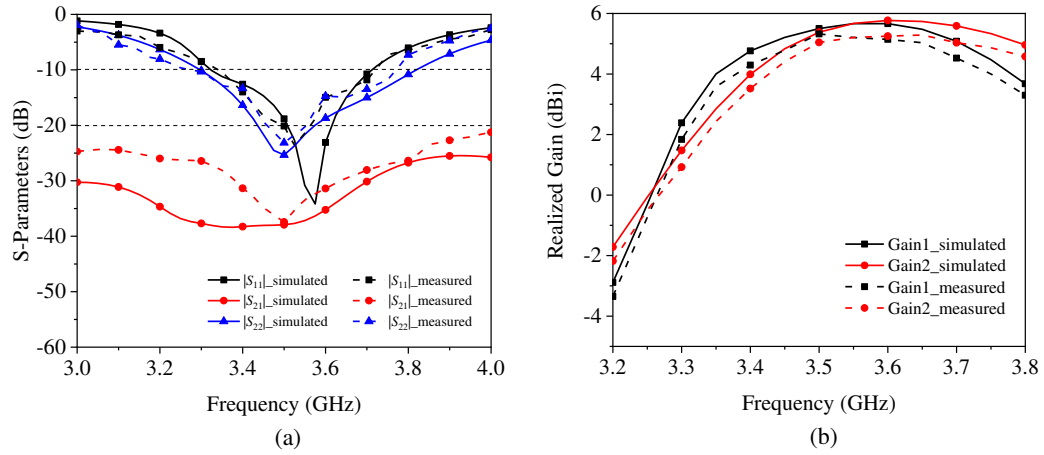

Figure 11. Simulated and measured: (a) S-parameters, (b) realized gain.

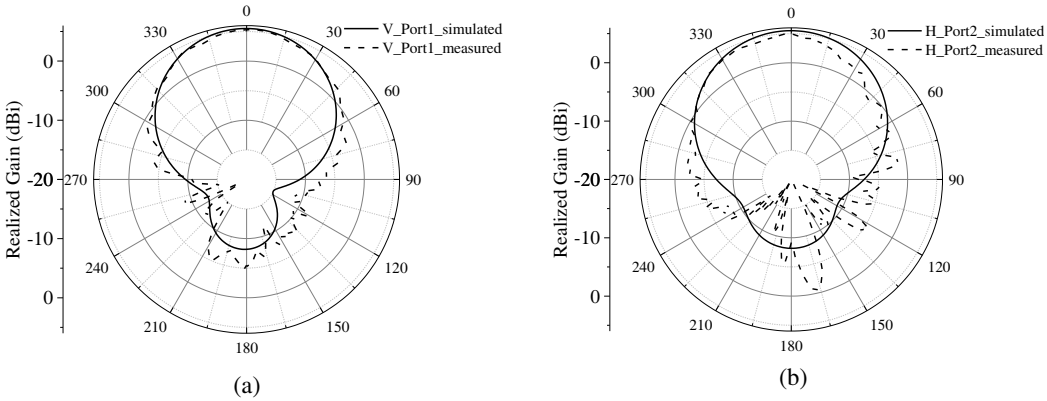

Figure 12. Simulated and measured radiation patterns at 3.5 GHz: (a) Vertical polarization port, (b) horizontal polarization port.

Table 2. Comparison of the related work.

Ref.	Freq. (GHz)	Electrical size	$\lvert S_{21}\rvert$ (dB)	Gain (dBi)
[7]	3.20–3.85	$1.3\lambda_0 \times 1.3\lambda_0 \times 0.12\lambda_0$	< -25	7.9
[8]	3.30–3.60	$0.84\lambda_0 \times 0.84\lambda_0 \times 0.14\lambda_0$	< -25	8.5
[9]	3.23–3.80	$0.84\lambda_0 \times 0.84\lambda_0 \times 0.4\lambda_0$	< -23	8.9
[10]	3.20–3.86	$0.3\lambda_0 \times 0.3\lambda_0 \times 0.21\lambda_0$	< -25	7.3
Prop.	3.24–3.66	$0.45\lambda_0 \times 0.45\lambda_0 \times 0.18\lambda_0$	< -35	5.3

4. CONCLUSION

In this paper, a hybrid-fed dual-polarized antenna that can be used as a 5G mobile communication base station antenna is proposed. By placing the two feeding ports orthogonally on different layers of dielectric plates and using electromagnetic coupling and gap coupling for feeding respectively, the port isolation is greatly improved. In addition, a metasurface coverage unit is loaded above the patch to achieve broadband and high gain characteristics. The measurement results show that the antenna has an impedance bandwidth of 12% (3.24 to 3.66 GHz). In addition, a stable gain about 5.32 dBi was obtained at 3.5 GHz. The simulated and measured results are in great agreement to verify the proposed antenna.

Table 2 lists the performances of proposed work and some other similar works, which are designed to operate in the 5G band. As can be seen from Table 2, the proposed antenna outperforms the cited research particularly in size and isolation and can be a good candidate for application in 5G base station systems.

ACKNOWLEDGMENT

This work was supported in part by the Jiangsu Agriculture Science and Technology Innovation Fund (JASTIF; Project number: CX(21)3187), and in part by the National Natural Science Foundation of China under Grant 62101266.

REFERENCES

1. Jin, H., L. Zhu, H. Zou, et al., "A wideband dual-polarized antenna and its array with electrically downtilt function for 5G sub-6 GHz communication applications," *IEEE Access*, Vol. 8, 7672–7681, 2020.
2. Carver, K. and J. Mink, "Microstrip antenna technology," *IEEE Trans. Antennas Propag.*, Vol. 29, No. 1, 2–24, Apr. 2003.
3. Cui, Y. H., R. L. Li, and H. Z. Fu, "A broadband dual-polarized planar antenna for 2G/3G/LTE base stations," *IEEE Trans. Antennas Propag.*, Vol. 62, No. 9, 4836–4840, Sep. 2014.
4. Gou, Y. S., S. W. Yang, J. X. Li, and Z. P. Nie, "A compact dual-polarized printed dipole antenna with high isolation for wideband base station applications," *IEEE Trans. Antennas Propag.*, Vol. 62, No. 8, 4392–4395, Aug. 2014.
5. Huang, H., Y. Liu, and S. X. Gong, "A broadband dual-polarized base station antenna with sturdy construction," *IEEE Antennas Wireless Propag. Lett.*, Vol. 16, 665–668, 2017.
6. Chung, Y., S. Jeon, D. Ahn, J. Choi, and T. Itoh, "High isolation dual-polarized patch antenna using integrated defected ground structure," *IEEE Microwave and Wireless Components Lett.*, Vol. 14, No. 1, 4–6, Jan. 2004.
7. Miran, E. A. and M. Ciydem, "Dual-polarized elliptic-H slot-coupled patch antenna for 5G applications," *Turkish Journal of Electrical Engineering and Computer Sciences*, Vol. 30, No. 4, 1204–1218, 2022.
8. Alieldin, Y. Huang, M. Stanley, S. D. Joseph, and D. Lei, "A 5G MIMO antenna for broadcast and traffic communication topologies based on pseudo inverse synthesis," *IEEE Access*, Vol. 6, 65935–65944, 2018.
9. Hua, C., R. Li, Y. Wang, and Y. Lu, "Dual-polarized filtering antenna with printed Jerusalem-cross radiator," *IEEE Access*, Vol. 6, 9000–9005, 2018.
10. Huang, H., X. P. Li, and Y. M. Liu, "5G MIMO antenna based on vector synthetic mechanism," *IEEE Antennas Wireless Propag. Lett.*, Vol. 17, 1052–1055, 2018.
11. Lin, F. H. and Z. N. Chen, "Low-profile wideband metasurface antennas using characteristic mode analysis," *IEEE Trans. Antennas Propag.*, Vol. 65, No. 4, 1706–1713, 2017.
12. Holloway, C. L., et al., "An overview of the theory and applications of metasurfaces: The two-dimensional equivalents of metamaterials," *IEEE Antennas and Propagation Magazine*, Vol. 54, No. 2, 10–35, 2012.
13. Zhang, L., et al., "Advances in full control of electromagnetic waves with metasurfaces," *Advanced Optical Materials*, Vol. 4, No. 6, 818–833, 2016.
14. Zhu, H. L., S. W. Cheung, X. H. Liu, and T. I. Yuk, "Design of polarization reconfgurable antenna using metasurface," *IEEE Trans. Antennas Propag.*, Vol. 62, No. 6, 2891–2898, Jun. 2014.
15. Liu, W., et al., "Metamaterial-based low-profile broadband aperture-coupled grid-slotted patch antenna," *IEEE Trans. Antennas Propag.*, Vol. 63, No. 7, 3325–3329, Jun. 2015.
16. Croq, F. and D. M. Pozar, "Millimeter-wave design of wide-band aperture-coupled stacked microstrip antennas," *IEEE Trans. Antennas Propag.*, Vol. 39, No. 12, 1770–1776, Apr. 1991.